

# EXPLORING THE IMPACT OF PLASMONIC METALS ON THE PROPERTIES OF PLASMONIC METAL + TiO<sub>2</sub> CATALYSTS

*Špela Slapničar, Gregor Žerjav, Albin Pintar*  
National Institute of Chemistry, Ljubljana, Slovenia  
E-mail: spela.slapnicar@ki.si

## ABSTRACT

In this work, the use of plasmonic metals deposited on hydrothermally synthesized TiO<sub>2</sub> nanorods (TNR) as catalysts was investigated. The plasmonic metals (PM) used were Au, Ag and Pt at a concentration of 1.0 wt.%. The prepared solids were systematically characterized to evaluate their structural, optical and electronic properties. The UV-Vis diffuse reflectance spectra consistently showed absorption peaks indicating the presence of metallic nanoparticles (NPs). The TNR-PM catalysts generated superoxide anion and hydroxyl radicals, which was confirmed by reactive oxygen radical formation tests. The photocatalytic activity was evaluated by the degradation of the model organic pollutant bisphenol A (BPA).

**Key words:** heterogeneous photocatalysis, titanium dioxide, plasmonic metals, wastewater purification

## INTRODUCTION

TiO<sub>2</sub> stands out as one of the most commonly utilized semiconducting oxides, prized for its versatility in heterogeneous photocatalysis. However, its significant drawback lies in its wide band gap of 3.2 eV, restricting activation solely to UV light. The strategic deposition of plasmonic metallic (PM) nanoparticles, such as Au, Ag, and Pt, onto TiO<sub>2</sub> surfaces holds promise in harnessing visible light and near-infrared radiation from the solar spectrum [1,2]. Hence, the primary objective of this study was to comprehensively investigate the impact of plasmonic metal deposition on the properties of TNR-PM catalysts. Furthermore, the study aimed to evaluate their effectiveness in generating reactive oxygen species under visible-light exposure. Additionally, the synthesized TNR-PM solids were tested for their suitability in wastewater purification via advanced oxidation processes (AOPs) conducted under visible-light illumination in a batch slurry reactor, employing the endocrine-disrupting compound bisphenol A (BPA) as a model organic pollutant.

## EXPERIMENTAL

Titanate nanorods (TNR) were synthesized using the hydrothermal method, with the procedure outlined in our previous publications [3,4]. The wet impregnation technique was employed to deposit plasmonic metal (PM) nanoparticles onto the TNR surface. Initially, TNR were dispersed in ethanol via ultrasonication. Subsequently, either (i) 10 mM HAuCl<sub>4</sub>, (ii) 10 mM AgNO<sub>3</sub> aqueous solution, or (iii) a 3.4 wt.% Pt(NH<sub>3</sub>)<sub>2</sub>(NO<sub>2</sub>)<sub>2</sub> solution in dilute ammonium hydroxide was added to the TNR/ethanol mixture and stirred for 2 hours. Following drying at 80 °C for 18 hours, the resulting materials underwent calcination at 300 °C in a 5% H<sub>2</sub>/95% N<sub>2</sub> gas atmosphere with a heating ramp of 150 °C/h [5]. To evaluate the photocatalytic activity of investigated TNR-PM catalysts, we performed a series of experiments to determine the oxidation pathway of the water-dissolved model organic pollutant bisphenol A (BPA). We further performed tests with 2,2'-azino-bis(3-ethylbenzothiazoline-6-sulfonic acid cation (ABTS<sup>+</sup>) and coumarin (COUM), acting as radical scavengers, to measure the visible-light triggered generation rates of different ROS (i.e. superoxide anion O<sub>2</sub><sup>•-</sup> and OH<sup>•</sup> radicals). The catalytic reaction for BPA degradation was carried out in a glass batch slurry reactor at a

constant temperature of 25 °C. The suspension with BPA ( $c_0=10.0$  mg/L) and catalysts ( $c_{cat}=125$  mg/L) was first stirred in the dark for 20 minutes to establish sorption equilibrium and then the visible-light source was switched on.

## RESULTS AND DISCUSSION

The wet impregnation technique resulted three distinct catalysts, each exhibiting a plasmonic metal loading of approximately 1.0 wt.%, as indicated by SEM-EDXS analysis listed in Table 1. Furthermore, the EDXS analysis proves that no residues of PM precursors are present in the samples. The TEM micrographs reveal that the catalysts predominantly adopt a nanorod morphology for TiO<sub>2</sub>, as anticipated. In addition, the PM nanoparticles have a spherical shape and different sizes. Notably, the TNR+Pt sample displays the narrowest particle size distribution and the smallest Pt particles, while Au exhibits the largest particles. N<sub>2</sub> physisorption results show that the specific surface area ( $S_{BET}$ ), pore volume ( $V_{pore}$ ) and pore diameter ( $d_{pore}$ ) on the TNR+PM catalysts were mainly dominated by the TNR support, as summarized in Table 1. Minimal changes in catalyst properties indicate the stability of TNR during wet impregnation. XRD analysis yielded diffractograms, with the anatase crystallite size calculated using the Scherrer equation showing a uniform size of 17.4 nm for all materials studied.

Table 1. Results of the SEM-EDXS, N<sub>2</sub> adsorption/desorption and TEM analyses of the investigated TNR support and TNR-PM catalysts.

SAMPLE		TNR	TNR+Au	TNR+Ag	TNR+Pt
SEM-EDXS (wt.%)	Ti	49.2±2.0	53.5±2.1	54.7±3.3	51.9±3.0
	O	50.8±2.0	45.7±2.1	44.4±3.3	47.1±3.0
	Au	-	0.8±0.1	-	-
	Ag	-	-	1.0±0.1	-
	Pt	-	-	-	1.0±0.1
$S_{BET}$ (m <sup>2</sup> /g)		106	105	106	108
$V_{pore}$ (cm <sup>3</sup> /g)		0.48	0.47	0.48	0.47
$d_{pore}$ (nm)		18.3	17.9	17.4	17.1
PM average size (nm)		-	49.8	5.2	1.5

The UV-Vis DR spectra (Fig. 1) show light absorption in the UV range (below 400 nm) and remarkable absorption peaks for Au particles in the visible range (hump at 550 nm). Ag LSPR occurs between 350-400 nm for nanoparticles below 10 nm, which is the reason why there is no hump in the visible range. Interestingly, the TNR-Pt and TNR-Ag samples have a higher absorption in the visible range. It is possible to have electronic excitations from filled s-states below the Fermi level to empty states above the Fermi level, known as intraband transitions. These excitations are generally present in all transition metals in the visible region [6]. Using solid-state photoluminescence (PL), the TNR sample was found to have a high PL intensity, indicating a high recombination rate of charge carriers. The PL curves of samples with PM nanoparticles deposited on TNR show low intensity as there is less emissive recombination in the samples. This enhancement contributes to improved photocatalytic activity of TNR-PM photocatalysts compared to bare TNR.

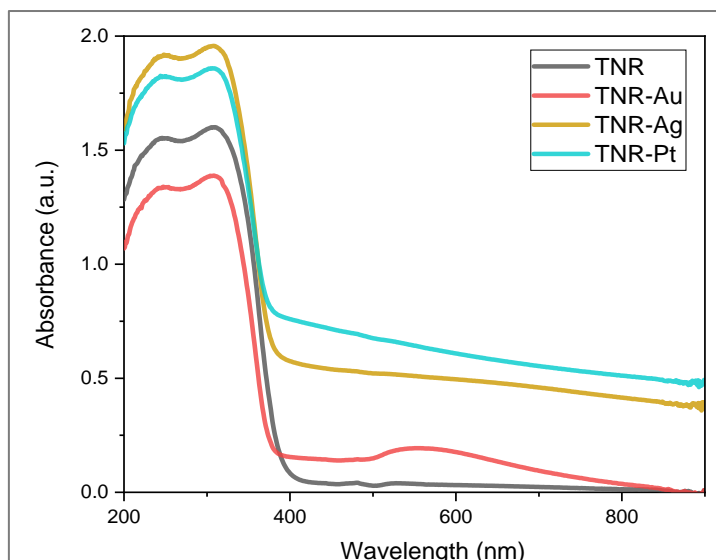


Figure 1. UV/Vis DR spectra of examined solids.

Tests were performed with  $\text{ABTS}^{\bullet+}$  and COUM solutions to observe the development of ROS. The results for the bare TNR (without PM) show that no  $\text{OH}^{\bullet}$  and  $\text{O}_2^{\bullet-}$  radicals are formed, as the reactions take place under visible light, where  $\text{TiO}_2$  is inactive. It is noteworthy that the TNR-Pt sample showed the fastest evolution of 7-hydroxycoumarin, indicating a better formation of  $\text{OH}^{\bullet}$  radicals compared to the other samples, while the TNR+Ag sample showed the least formation of  $\text{OH}^{\bullet}$  radicals. In another reaction with  $\text{ABTS}^{\bullet+}$ ,  $e^-$  in the conduction band and the formation of  $\text{O}_2^{\bullet-}$  were observed. Again, the TNR-Pt sample showed the highest  $\text{ABTS}^{\bullet+}$  reduction rate, while the TNR-Au sample showed the lowest. In the photocatalytic oxidation of an aqueous BPA solution, no adsorption of BPA was observed in any of the tested materials during the dark phase (grey area). The photocatalytic activity of the bare TNR can be attributed to the presence of  $\text{Ti}^{3+}$  species on the surface and/or surface defects. Remarkably, the TNR-Pt sample showed the highest degradation rate under visible light, achieving almost 70 % BPA degradation within 2 hours (Fig. 2).

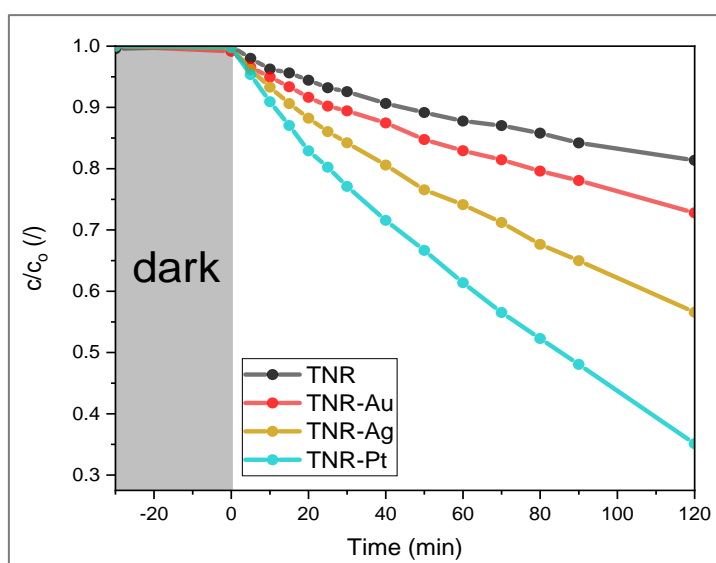


Figure 2. BPA degradation obtained in the presence of prepared photocatalysts. Experimental conditions:  $c_0(\text{BPA})=10.0 \text{ mg/L}$ ,  $T=25 \text{ }^\circ\text{C}$ ,  $c_{\text{cat}}=125 \text{ mg/L}$ .

## CONCLUSION

SEM-EDXS analysis revealed that all synthesized samples contained 1 wt.% PM. Furthermore, N<sub>2</sub> physisorption analysis of the TNR-PM catalysts showed minimal changes compared to bare TNR, indicating that the presence of 1 wt.% PM does not clog the pores of the TNR. The UV-Vis DR spectra of the investigated TNR-PM materials showed light absorption by the TNR support in the UV light region, while the absorption of the PM particles occurred in the visible-light region due to the localized surface plasmon resonance effect. Solid-state PL measurements revealed that the PL intensity and the recombination rate of charge carriers were similar for all TNR-PM catalysts and lower compared to bare TNR. The results of the reactive oxygen species formation tests confirmed the ability of TNR-PM catalysts to generate charge carriers under visible-light illumination. The analysis of the BPA degradation results showed different photocatalytic degradation activities of the different PMs. The TNR-Pt sample showed both the highest charge carrier generation and the highest BPA conversion rate, while the TNR-Au sample showed the lowest BPA conversion rate. These differences in degradation can be attributed to the different sizes of PM particles, as smaller and uniformly distributed PMs are known to be more active. The consistently observed trends in the catalytic activity of the TNR-PM catalysts indicate that the primary oxidation pathway of BPA degradation involves superoxide anion radicals.

## REFERENCES

- [1] G. Žerjav, J. Zavašnik, J. Kovač, A. Pintar, The influence of Schottky barrier height onto visible-light triggered photocatalytic activity of TiO<sub>2</sub>+Au composites, *Appl. Surf. Sci.*, 2021, 543, 148799.
- [2] G. Žerjav, A. Albreht, I. Vovk, A. Pintar, Revisiting terephthalic acid and coumarin as probes for photoluminescent determination of hydroxyl radical formation rate in heterogeneous photocatalysis, *Appl. Catal. A*, 2021, 598, 117566.
- [3] G. Žerjav, M.S. Arshad, P. Djinović, J. Zavašnik, A. Pintar, Electron trapping energy states of TiO<sub>2</sub>-WO<sub>3</sub> composites and their influence on photocatalytic degradation of bisphenol A, *Appl. Catal. B*, 2017, 209, 273-284.
- [4] G. Žerjav, M.S. Arshad, P. Djinović, I. Junkar, J. Kovač, J. Zavašnik, A. Pintar, Improved electron-hole separation and migration in anatase TiO<sub>2</sub> nanorod/reduced graphene oxide composites and their influence on photocatalytic performance, *Nanoscale*, 2017, 9, 4578-4592.
- [5] P. Verma, K. Mori, Y. Kuwahara, S.J. Cho, H. Yamashita, Synthesis of plasmonic gold nanoparticles supported on morphology-controlled TiO<sub>2</sub> for aerobic alcohol oxidation, *Catal. Today*, 2020, 352, 255-261.
- [6] U. Aslam, V.G. Rao, S. Chavez, S. Linic, Catalytic conversion of solar to chemical energy on plasmonic metal nanostructures, *Nature Catal.*, 2018, 1, 656-665.